

The Thermodynamics of Slow Invariant Manifolds for Reactive Systems

J. M. Powers, S. Paolucci

University of Notre Dame, Department of Aerospace and Mechanical Engineering, Notre Dame, Indiana, USA

Abstract—Construction of the Slow Invariant Manifold (SIM) for a reactive system is coming to be realized as the linchpin in a rational method of reduced kinetics. Here a method of constructing a finite dimensional SIM based on identifying critical points and connecting them with trajectories is shown for a spatially homogeneous reactive system. The relation between this analysis and classical as well as irreversible thermodynamics is examined.

I. INTRODUCTION

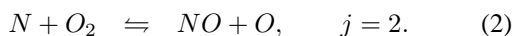
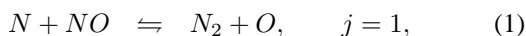
Two common problems arise in manifold methods: 1) their calculation can be difficult, and 2) they only form an approximation in a limited range to the more useful SIM of the system. We extend here the development of a method suggested to us by Davis and Skodje [1]: calculation of the SIM by integration from various finite and infinite critical points to the stable node of the physical equilibrium. We consider a simple but realistic detailed kinetic system. The method requires identification of *all equilibria* of ordinary differential equations (ODEs) describing the time-evolution dynamics of spatially homogeneous systems. Some of these roots will lie in non-physical regions of chemical composition space; nevertheless, they provide the seed for the growth of the SIM, which describes the long time dynamics of the chemical system as it approaches the equilibrium state. A important goal is to carefully expose the links between classical thermodynamics, the non-equilibrium thermodynamics of chemical kinetics, and modern mathematical theory of non-linear dynamics on model problems.

II. MODEL PROBLEM

We illustrate our approach for calculating the SIM by applying it to important problems in reaction kinetics. One the mechanisms to be discussed is the Zel'dovich mechanism of formation of nitric oxide. We consider the special case in which the reaction is isothermal and isobaric. This kinetic model is widely used, is simple enough that its exposition remains compact, and rich enough to reveal some of the complexities of multiple equilibria, chemical stiffness, and a non-trivial SIM.

A. Reaction Mechanism

The reaction mechanism describes how $M = 5$ molecular species, NO , N , N_2 , O , and O_2 , composed of $L = 2$ atomic elements, N and O , react in $J = 2$ reversible reactions:



These two reactions proceed according to the law of mass action, with a rate modulated by an Arrhenius temperature-dependency. The reaction rates are

$$r_1 = \alpha_1 T^{\beta_1} e^{-\frac{T_{a,1}}{T}} \bar{\rho}_N \bar{\rho}_{NO} \left(1 - \frac{1}{K_{c,1}^{eq}} \frac{\bar{\rho}_{N_2} \bar{\rho}_O}{\bar{\rho}_N \bar{\rho}_{NO}} \right) \quad (3)$$

$$r_2 = \alpha_2 T^{\beta_2} e^{-\frac{T_{a,2}}{T}} \bar{\rho}_N \bar{\rho}_{O_2} \left(1 - \frac{1}{K_{c,2}^{eq}} \frac{\bar{\rho}_{NO} \bar{\rho}_O}{\bar{\rho}_N \bar{\rho}_{O_2}} \right). \quad (4)$$

Variables are, for $j = 1, 2$, the reaction rates, r_j , and for $i = 1, \dots, 5$, the molecular species molar concentrations $\bar{\rho}_i$. We interchangeably employ conventional chemistry notation for species molar concentration, e.g. $\bar{\rho}_N = [N]$. Constant parameters, for an *isothermal* reaction, are the collision frequency factor α_j , the temperature T , the temperature-sensitivity exponent β_j , the activation temperature $T_{a,j}$, and the equilibrium constant $K_{c,j}^{eq}$. Equilibrium thermochemistry shows how to determine $K_{c,j}^{eq}$ in terms of more fundamental thermodynamic quantities. These standard relations are

$$K_{c,j}^{eq} = \left(\frac{P_o}{RT} \right)^{\sum_{i=1}^M \nu_{i,j}} \exp \left(\frac{-\Delta G_j^o}{RT} \right), \quad j = 1, 2. \quad (5)$$

Here, $P_o = 1 \times 10^6 \text{ dyne/cm}^2$ is the reference pressure, \bar{R} is the universal gas constant, $\sum_{i=1}^M \nu_{i,j}$ is the net change of moles in reaction j , and ΔG_j^o is the change in Gibbs free energy at the reference pressure for the j^{th} reaction. Gibbs free energy changes at the reference pressure are

$$\Delta G_1^o = \bar{g}_{N_2}^o + \bar{g}_O^o - \bar{g}_N^o - \bar{g}_{NO}^o, \quad (6)$$

$$\Delta G_2^o = \bar{g}_{NO}^o + \bar{g}_O^o - \bar{g}_N^o - \bar{g}_{O_2}^o. \quad (7)$$

Above, \bar{g}_i^o is the partial molar Gibbs free energy of species i at the reference pressure. This can be determined by using the definition of Gibbs free energy at the reference pressure, $\bar{g}_i^o = \bar{h}_i^o - T \bar{s}_i^o$, where \bar{h}_i^o and \bar{s}_i^o are the partial molar enthalpy and entropy at the reference pressure, respectively. Now, take $T = 6000 \text{ K}$, an elevated temperature for gas phase reactions. Next, employing thermodynamic data from Sonntag, *et al.* [2], and kinetic data from Baulch, *et al.* [3], the kinetic rates r_j from Eqs. (3-4) can be numerically specified. The individual molecular species evolve according to Eqs. (1-2) at the rates dictated by Eqs. (3-4). Their evolution is

described by the ODEs and initial conditions:

$$\frac{d\bar{\rho}_{NO}}{dt} = \omega_{NO} \equiv -r_1 + r_2, \quad \bar{\rho}_{NO}(0) = \bar{\rho}_{NO}^*, \quad (8)$$

$$\frac{d\bar{\rho}_N}{dt} = \omega_N \equiv -r_1 - r_2, \quad \bar{\rho}_N(0) = \bar{\rho}_N^*, \quad (9)$$

$$\frac{d\bar{\rho}_{N_2}}{dt} = \omega_{N_2} \equiv r_1, \quad \bar{\rho}_{N_2}(0) = \bar{\rho}_{N_2}^*, \quad (10)$$

$$\frac{d\bar{\rho}_O}{dt} = \omega_O \equiv r_1 + r_2, \quad \bar{\rho}_O(0) = \bar{\rho}_O^*, \quad (11)$$

$$\frac{d\bar{\rho}_{O_2}}{dt} = \omega_{O_2} \equiv -r_2. \quad \bar{\rho}_{O_2}(0) = \bar{\rho}_{O_2}^*. \quad (12)$$

Quantities with a * superscript denote the initial state, and ω_i is the species production rate for species i . Equations (8-12) augmented by Eqs. (3-4) form five ODEs in five unknowns.

B. Conserved Quantities

1) *Element Conservation*: Chemical reactions are characterized by the property that the total number of elements remains constant. For the element N , this is exhibited by the the following linear combination of Eqs. (8-10):

$$\frac{d\bar{\rho}_{NO}}{dt} + \frac{d\bar{\rho}_N}{dt} + 2\frac{d\bar{\rho}_{N_2}}{dt} = 0. \quad (13)$$

Equation (13) can be integrated to form the relation

$$\bar{\rho}_{NO} + \bar{\rho}_N + 2\bar{\rho}_{N_2} = \bar{\rho}_{NO}^* + \bar{\rho}_N^* + 2\bar{\rho}_{N_2}^*. \quad (14)$$

Similarly for O , using Eqs. (8,11,12), one finds

$$\bar{\rho}_O + \bar{\rho}_{NO} + 2\bar{\rho}_{O_2} = \bar{\rho}_O^* + \bar{\rho}_{NO}^* + 2\bar{\rho}_{O_2}^*. \quad (15)$$

2) *Molecule Conservation*: Generally, the number of molecules is not constant in chemical reactions. However, it is the case in the Zel'dovich mechanism, and this provides an additional algebraic constraint. By adding Eqs. (8-12) and then integrating, one finds

$$\bar{\rho}_{NO} + \bar{\rho}_N + \bar{\rho}_{N_2} + \bar{\rho}_O + \bar{\rho}_{O_2} = \bar{\rho}_{NO}^* + \bar{\rho}_N^* + \bar{\rho}_{N_2}^* + \bar{\rho}_O^* + \bar{\rho}_{O_2}^*. \quad (16)$$

3) *Linear Dependencies*: Equations (14-16) form an under-constrained linear system. We can select $\bar{\rho}_{NO}$ and $\bar{\rho}_N$ as primary dependent variables and use the linear system to cast the secondary dependent variables, $\bar{\rho}_{N_2}$, $\bar{\rho}_O$, and $\bar{\rho}_{O_2}$, in terms of the primary via Gaussian elimination:

$$\bar{\rho}_{N_2} = \frac{1}{2} (2\bar{\rho}_{N_2}^* + \bar{\rho}_N^* + \bar{\rho}_{NO}^* - \bar{\rho}_N - \bar{\rho}_{NO}), \quad (17)$$

$$\bar{\rho}_O = \bar{\rho}_N^* - 2\bar{\rho}_{O_2}^* - \bar{\rho}_O^* - \bar{\rho}_N, \quad (18)$$

$$\bar{\rho}_{O_2} = \frac{1}{2} (-\bar{\rho}_N^* + \bar{\rho}_{NO}^* + 4\bar{\rho}_{O_2}^* + 2\bar{\rho}_O^* + \bar{\rho}_N - \bar{\rho}_{NO}). \quad (19)$$

C. Final Form

For convenience, we select the set of initial concentrations $\bar{\rho}_{NO}^* = \bar{\rho}_N^* = \bar{\rho}_{N_2}^* = \bar{\rho}_O^* = \bar{\rho}_{O_2}^* = 10^{-3} \text{ mole/cm}^3$. This gives rise to a pressure of $P = 2.5 \times 10^6 \text{ dyne/cm}^2$. Then, using Eqs. (3-8, 17-19), the reaction rates ω_{NO} and ω_N become

$$\omega_{NO} = 7.2 \times 10^{-1} - 2.2 \times 10^7 \bar{\rho}_N + 1.1 \times 10^{13} \bar{\rho}_N^2 - 9.4 \times 10^5 \bar{\rho}_{NO} - 3.2 \times 10^{13} \bar{\rho}_N \bar{\rho}_{NO}, \quad (20)$$

$$\omega_N = 7.2 \times 10^{-1} - 2.3 \times 10^7 \bar{\rho}_N - 1.1 \times 10^{13} \bar{\rho}_N^2 + 5.8 \times 10^5 \bar{\rho}_{NO} - 1.0 \times 10^{13} \bar{\rho}_N \bar{\rho}_{NO}. \quad (21)$$

These initial conditions are chosen arbitrarily to illustrate the technique. Thus, we obtain two non-linear ODEs in the two unknowns, $\bar{\rho}_{NO}, \bar{\rho}_N$:

$$\frac{d\bar{\rho}_{NO}}{dt} = \omega_{NO}(\bar{\rho}_{NO}, \bar{\rho}_N), \quad \bar{\rho}_{NO}(0) = 10^{-3} \frac{\text{mole}}{\text{cm}^3}, \quad (22)$$

$$\frac{d\bar{\rho}_N}{dt} = \omega_N(\bar{\rho}_{NO}, \bar{\rho}_N), \quad \bar{\rho}_N(0) = 10^{-3} \frac{\text{mole}}{\text{cm}^3}. \quad (23)$$

D. Equilibria

Equations (22-23) have equilibrium points $(\bar{\rho}_{NO}^e, \bar{\rho}_N^e)$ where $\omega_{NO} = 0$ and $\omega_N = 0$. One of these equilibria is that typically identified by traditional thermochemistry and can be associated with a minimization of the Gibbs free energy. Others exist, which are non-physical because of either negative or infinite molar concentrations. However, as demonstrated by Ref. [1], identification of non-physical equilibria is a critical step in the construction of the useful one-dimensional SIM. For Eqs. (22-23), five roots, R_1, R_2, R_3, R_4 , and R_5 , are found:

$$R_1 = (\bar{\rho}_{NO}^e, \bar{\rho}_N^e) = (7.3 \times 10^{-7}, 3.7 \times 10^{-8}), \quad (24)$$

$$R_2 = (\bar{\rho}_{NO}^e, \bar{\rho}_N^e) = (-1.6 \times 10^{-6}, -3.1 \times 10^{-8}), \quad (25)$$

$$R_3 = (\bar{\rho}_{NO}^e, \bar{\rho}_N^e) = (-5.2 \times 10^{-8}, -2.0 \times 10^{-6}), \quad (26)$$

$$R_4 = (\bar{\rho}_{NO}^e, \bar{\rho}_N^e) = (+\infty, 0), \quad (27)$$

$$R_5 = (\bar{\rho}_{NO}^e, \bar{\rho}_N^e) = (-\infty, 0). \quad (28)$$

Numerical values above all have units of mole/cm^3 . Only R_1 is physical. The roots at infinity are identified via the standard method discussed by Perko [4]. It is easily shown that the equilibria are precisely those found by means of traditional chemistry: setting each reaction rate to zero, $r_1 = r_2 = 0$, and thus demanding, from Eqs. (3,4), that

$$K_{c,1}^{eq} = \frac{\bar{\rho}_{N_2} \bar{\rho}_O}{\bar{\rho}_N \bar{\rho}_{NO}}, \quad K_{c,2}^{eq} = \frac{\bar{\rho}_{NO} \bar{\rho}_O}{\bar{\rho}_N \bar{\rho}_{O_2}}. \quad (29)$$

Equations (29), in conjunction with the element constraints, Eqs. (17-19), form five equations in five unknowns. These have exactly the same roots as those found by setting $\omega_{NO} = 0$, $\omega_N = 0$.

E. Linear Stability

The dynamics of Eqs. (22,23) are elucidated by studying their behavior near each of the equilibria. Using standard linearization techniques, Eqs. (22,23) near the finite equilibrium points behave as

$$\frac{d}{dt} \begin{pmatrix} \bar{\rho}_{NO} - \bar{\rho}_{NO}^e \\ \bar{\rho}_N - \bar{\rho}_N^e \end{pmatrix} = \underbrace{\begin{pmatrix} \frac{\partial \omega_{NO}}{\partial \bar{\rho}_{NO}} \Big|_{\bar{\rho}_{NO}^e, \bar{\rho}_N^e} & \frac{\partial \omega_{NO}}{\partial \bar{\rho}_N} \Big|_{\bar{\rho}_{NO}^e, \bar{\rho}_N^e} \\ \frac{\partial \omega_N}{\partial \bar{\rho}_{NO}} \Big|_{\bar{\rho}_{NO}^e, \bar{\rho}_N^e} & \frac{\partial \omega_N}{\partial \bar{\rho}_N} \Big|_{\bar{\rho}_{NO}^e, \bar{\rho}_N^e} \end{pmatrix}}_{\equiv \mathbf{J}} \begin{pmatrix} \bar{\rho}_{NO} - \bar{\rho}_{NO}^e \\ \bar{\rho}_N - \bar{\rho}_N^e \end{pmatrix} \quad (30)$$

The Jacobian matrix \mathbf{J} acquires a numerical value at each finite equilibrium. Its eigenvalues, λ_j , determine the stability. Magnitudes of the reciprocals of each λ_j provide the time scales of evolution, τ_j , near the equilibrium. The eigenvalues associated with each finite equilibrium, R_1 , R_2 , R_3 , are

$$R_1 : (\lambda_1, \lambda_2) = (-1.2 \times 10^7, 5.4 \times 10^6), \quad (31)$$

$$R_2 : (\lambda_1, \lambda_2) = (4.4 \times 10^7 \pm 8.0 \times 10^6 i), \quad (32)$$

$$R_3 : (\lambda_1, \lambda_2) = (-3.1 \times 10^7, -2.1 \times 10^6). \quad (33)$$

The units for each eigenvalue are s^{-1} . The time constants for each equilibria are

$$R_1 : (\tau_1, \tau_2) = (8.4 \times 10^{-8} \text{ s}, 1.8 \times 10^{-7} \text{ s}), \quad (34)$$

$$R_2 : (\tau_1, \tau_2) = (2.3 \times 10^{-8} \text{ s}, 2.1 \times 10^{-8} \text{ s}), \quad (35)$$

$$R_3 : (\tau_1, \tau_2) = (3.2 \times 10^{-8} \text{ s}, 4.7 \times 10^{-7} \text{ s}). \quad (36)$$

The physical root R_3 is stable, and the two finite non-physical roots are unstable. For R_2 , with complex eigenvalues, τ_1 is associated with amplitude growth, and τ_2 is associated with oscillation time. The fastest time scale associated with the physical root, $\tau_1 = 3.2 \times 10^{-8} \text{ s}$ has been shown to be closely linked to the molecular collision time (Powers and Paolucci, [5]). Furthermore, the ratio of time scales for the physical root near equilibrium is $\tau_2/\tau_1 = 1.4 \times 10^1$. This gives evidence that even the two-step Zel'dovich mechanism retains stiffness at the elevated temperature, and that more general models which incorporate such kinetics will pose great computational challenges. For ordinary combustion temperatures, $\sim 1400 \text{ K}$, the stiffness ratio for the Zel'dovich mechanism dramatically increases to $\sim 10^6$. There are complications in analyzing the stability of roots at infinity, including fundamentally non-linear behavior. Numerical experiment suggests that R_4 is an unstable sink/saddle combination, and R_5 is an unstable source.

F. Non-Linear Dynamics

The full dynamics of the evolution of the concentrations as predicted by numerical integration are shown in Fig. 1. For early time, below the time scale of molecular collisions, the concentrations are unchanging. Near a time well predicted by the fast time scale $\tau_1 \sim 10^{-8} \text{ s}$ reaction events commence. At a time well predicted by the slow time scale $\tau_2 \sim 10^{-7} \text{ s}$, the system enters its final relaxation to the physical equilibrium, Eq. (33).

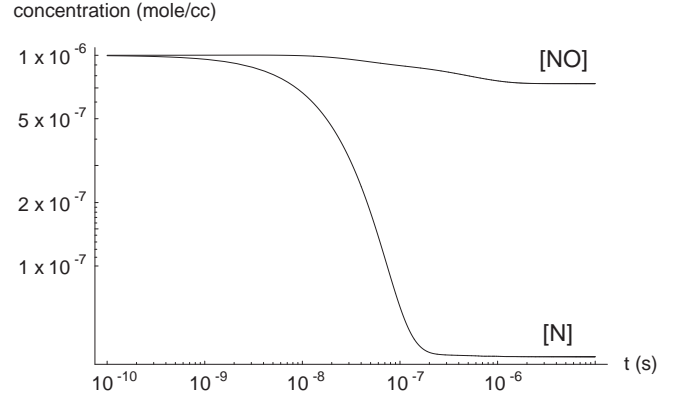


Fig. 1. Time evolution of concentrations for the isothermal Zel'dovich mechanism.

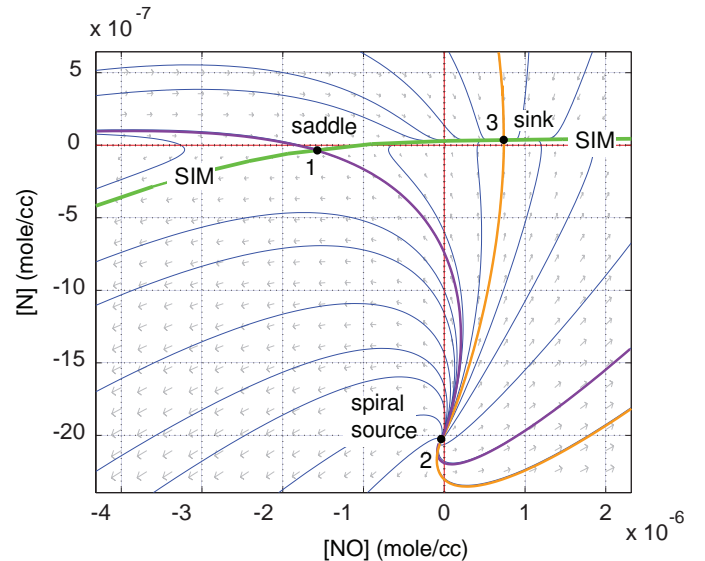


Fig. 2. Invariant manifold for the sample problem of an isothermal Zel'dovich mechanism.

G. Slow Invariant Manifold

One can obtain the important SIMs by numerically integrating Eqs. (22,23) from a critical point to another critical point, see Fig. 2, which focuses on the finite region of phase space. The curve labeled "SIM" is the slow invariant manifold; this is the set of points to which all reaction trajectories are attracted. Also shown are phase space trajectories for initial conditions that are close to the SIM. Numerical experiments allow one to map the trajectories on the so-called Poincaré sphere [4]. This allows one to project the roots at infinity in physical space onto a finite space and easily visualize the trajectories. Figure 3 gives a sketch of the trajectories in this projection. Because of scaling effects, it is difficult to graphically exhibit the behavior in the Poincaré projection; numerical experiments verify the topology shown here is correct.

While the phase space trajectory approaches an extremum of the Gibbs free energy near equilibrium, it is not certain why the path along the SIM is preferred.

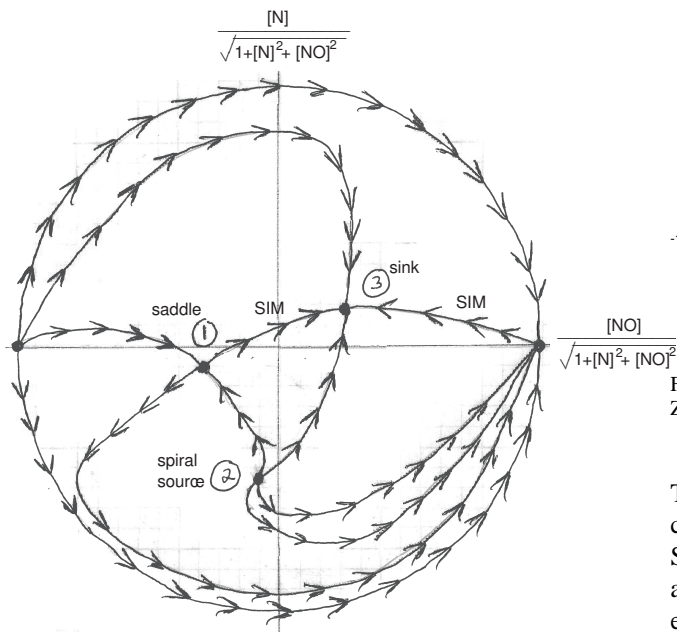


Fig. 3. Sketch of trajectories on projection of Poincaré sphere for the Zel'dovich mechanism.

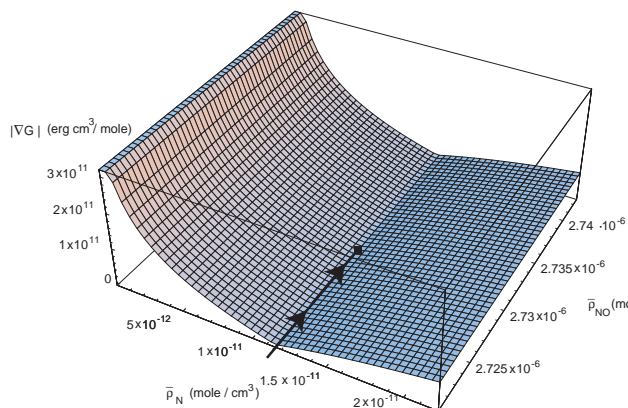


Fig. 4. Surface depicting $|\nabla G|$ near R_1 along with the trajectory of the slow invariant manifold for the sample problem of the isothermal Zel'dovich mechanism.

Consideration of the gradient of the Gibbs free energy allows an explanation to be formulated in the vicinity of the equilibrium point. Define the gradient of G in the \bar{p}_N, \bar{p}_{NO} phase space to be

$$\nabla G \equiv \begin{pmatrix} \left. \frac{\partial G}{\partial \bar{p}_{NO}} \right|_{\bar{p}_N} \\ \left. \frac{\partial G}{\partial \bar{p}_N} \right|_{\bar{p}_{NO}} \end{pmatrix}. \quad (37)$$

The magnitude is given by $|\nabla G| = \sqrt{\nabla G \cdot \nabla G}$. At equilibrium, $|\nabla G| = 0$. It takes on positive values away from the physical equilibrium. For the sample problem, the surface whose height is proportional to $|\nabla G|$ is shown in Fig. 4. There is an obvious valley in Fig. 4. It can be shown that this valley coincides with a valley in the gradient of the irreversibility production rate. Further comparison of the locus of this valley with the invariant manifold shows, near equilibrium, that they also coincide.

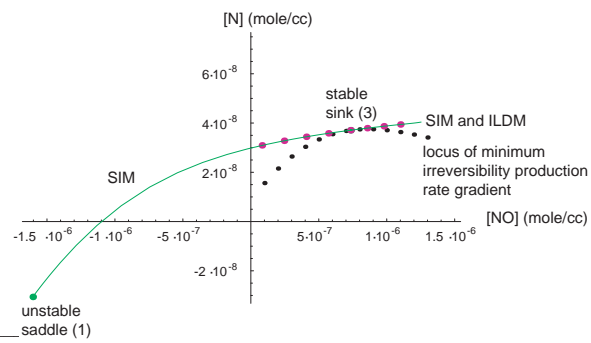


Fig. 5. Comparison of different theories for reduced kinetics in the Zel'dovich mechanism.

This behavior near equilibrium has led some to speculate, cf. Lebedz [6] that such a valley can elucidate the SIM far from the equilibrium point. This is not true, as can be seen in Fig. 5, which shows the SIM, an excellent approximation to the SIM given by the Maas-Pope Intrinsic Low Dimensional Manifold (ILDM), and a poor approximation away from equilibrium given by the locus of the minimum of the irreversibility production rate gradient. So two important questions are raised: 1) What is the connection between the SIM and thermodynamics? 2) What is the connection between dynamics of the system and its thermodynamics? These questions will be addressed in more detail.

III. CONCLUSION

The SIM is the key benchmark to which all methods of reduced kinetics can be compared. Its construction is aided by consideration of non-physical equilibria and points at infinity. While commonly used potentials such as the Gibbs free energy have some value in elucidating the dynamics near an equilibrium point, they offer no guidance for the behavior of the system far from equilibrium, where a more general formulation is required.

ACKNOWLEDGMENT

The authors recognize partial support of the National Science Foundation.

REFERENCES

- [1] Davis, M.J., and Skodje, R.T., 1999, Geometric investigation of low-dimensional manifolds in systems approaching equilibrium. *Journal of Chemical Physics*, **111**, pp. 859-874.
- [2] Sonntag, R.E., Borgnakke, C., and Van Wylen, J., 2002, *Fundamentals of Thermodynamics*, John Wiley, New York.
- [3] Baulch, D.L., Bowman, C.T., Cobos, C.J., Cox, R.A., Just, T., Kerr, J.A., Pilling, M.J., Stocker, D., Troe, J., Tsang, W., Walker, R.W., and Warnatz, J., 2005, "Evaluated kinetic data for combustion modeling: Supplement II," *Journal of Physical and Chemical Reference Data*, **34**, pp. 757-1397.
- [4] Perko, L., 2006, *Differential Equations and Dynamical Systems*, Third Edition, Springer-Verlag, Berlin.
- [5] Powers, J.M., and Paolucci, S., 2005, "Accurate spatial resolution estimates for reactive supersonic flow with detailed chemistry," *AIAA Journal*, **43**, pp. 1088-1099.
- [6] Lebedz, D., 2004, "Computing minimal entropy production trajectories: an approach to model reduction in chemical kinetics," *Journal of Chemical Physics*, **120**, pp. 6890-6897.